

Photoemission spectromicroscopy study of a $\text{Bi}_2\text{Sr}_2\text{CaCu}_2\text{O}_{8+\delta}$ single crystal

M. Bertolo,* S. La Rosa, A. Goldoni, and G. Cautero

Sincrotrone Trieste, S.S. 14 km 163.5-in Area Science Park, I-34012 Basovizza, Trieste, Italy

A. A. Zakharov

Max-Laboratory, Lund University, P.O. Box 118, S-22100, Lund, Sweden

I. Lindau

Department of Synchrotron Radiation Research, Lund University, P.O. Box 118, S-22100 Lund, Sweden

I. Vobornik

Laboratorio Nazionale TASC-INFN, S.S. 14 km 163.5, I-34012 Basovizza, Trieste, Italy

R. Yoshizaki

Institute of Applied Physics and Cryogenic Center, University of Tsukuba, Tsukuba, Ibaraki 305, Japan

(Received 26 March 2002; revised manuscript received 22 May 2002; published 16 August 2002)

We performed a photoemission microscopy study on cleaved surfaces of a $\text{Bi}_2\text{Sr}_2\text{CaCu}_2\text{O}_{8+\delta}$ single crystal. Our findings show that pronounced inhomogeneity effects exist even on good quality single crystals. The length scale of the observed features ranges from a few microns to a few hundred microns. We discuss the importance of our results for the interpretation of conventional photoemission experiments on $\text{Bi}_2\text{Sr}_2\text{CaCu}_2\text{O}_{8+\delta}$ which typically probe an area of the order of 1 mm^2 .

DOI: 10.1103/PhysRevB.66.060506

PACS number(s): 74.80.-g, 74.72.Hs, 79.60.-i

Shortly after the discovery of high- T_c superconductors,¹ it was recognized that the surface of these compounds is inhomogeneous. A high-resolution electron-energy-loss spectroscopy investigation, with a spatial resolution of the order of $50 \mu\text{m}$, demonstrated that both superconducting and nonsuperconducting areas coexist on the surface of cleaved $\text{YBa}_2\text{Cu}_3\text{O}_7$ and $\text{Bi}_2\text{Sr}_2\text{CaCu}_2\text{O}_8$ single crystals.² Inhomogeneities of the chemical composition were reported by scanning Auger microscopy studies of $\text{YBa}_2\text{Cu}_3\text{O}_{7-y}$ surfaces³ and by photoemission electron microscope investigations of $\text{HgBa}_2\text{Ca}_2\text{Cu}_3\text{O}_{8+\delta}$ and $\text{HgBa}_2\text{CaCu}_2\text{O}_{6+\delta}$ (Ref. 4) and single crystals of $\text{Bi}_2\text{Sr}_2\text{CaCu}_2\text{O}_{8+\delta}$.⁵ More recently, the importance of the availability of spatially resolving techniques has been demonstrated by a scanning photoemission microscopy study of $\text{Ba}_{1-x}\text{K}_x\text{BiO}_{3-y}$ single crystals.⁶

At the Spectromicroscopy beamline of ELETTRA,⁷ we performed a photoemission microscopy study on the cleaved surface of a $\text{Bi}_2\text{Sr}_2\text{CaCu}_2\text{O}_{8+\delta}$ single crystal. This technique uses the strength of the photoemission spectroscopic analysis, which probes the single-particle density of states. Here we put particular attention to the region close to the Fermi edge which is the important one for the superconductivity. This allows one to detect, with a submicron spatial resolution, variations of the electronic structure which are more subtle than topographical or chemical composition inhomogeneities and which would therefore be undetectable with other microscopy techniques.

The oxygen doping of the $\text{Bi}_2\text{Sr}_2\text{CaCu}_2\text{O}_{8+\delta}$ sample was close to optimum ($T_c = 91 \text{ K}$). More details about the sample and its characterization by low-energy electron diffraction (LEED) and angle-resolved photoelectron spectroscopy (ARPES) can be found in Ref. 8. The sample was cleaved and measured at room temperature. The photon energy used was 95 eV . The energy of the photoelectrons was analyzed

by a hemispherical analyzer with a 16-channel detector (the difference in energy between adjacent channels is 8% of the analyzer's pass energy). The images we present here are obtained by taking the counts of a single channel and are therefore associated to a given energy, or the sum of a few channels and are therefore associated to a given energy range. The photoelectrons were detected in the horizontal plane at 30° grazing angle from the sample surface with an acceptance of $\pm 5^\circ$. At the kinetic energy of the valence band, this gives $k_{\parallel} = 4.2 \pm 0.2 \text{ \AA}^{-1}$. By comparison with the size of the Brillouin zone ($\Gamma X \sim \Gamma Y \sim 1.16 \text{ \AA}^{-1}$) this corresponds to a fair degree of integration in the reciprocal space.

Figure 1 shows two photoemission images acquired at energies corresponding to the Bi $5d$ core level (from 25.90 to 26.06 eV below E_F) and to the valence band (from 3.36 to 4.56 eV below E_F), respectively. The image size is $45 \times 37 \mu\text{m}^2$. Three regions with different intensity levels, labeled A, B, and C, can be recognized in both images. The

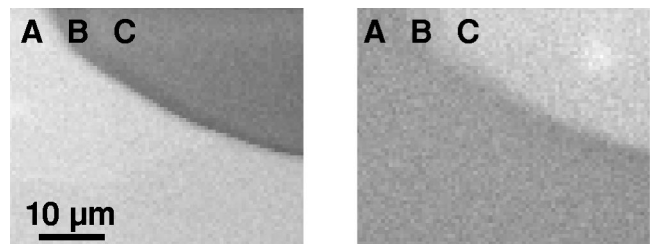


FIG. 1. Photoemission images of the cleaved surface of a $\text{Bi}_2\text{Sr}_2\text{CaCu}_2\text{O}_{8+\delta}$ single crystal. The size is $45 \times 37 \mu\text{m}^2$. The two images were acquired at energies corresponding to the Bi $5d$ level (left: from 25.90 to 26.06 eV below E_F) and to the valence band (right: from 3.36 to 4.56 eV below E_F), respectively. Three regions with different intensity levels, labeled A, B, and C, can be recognized in both images.

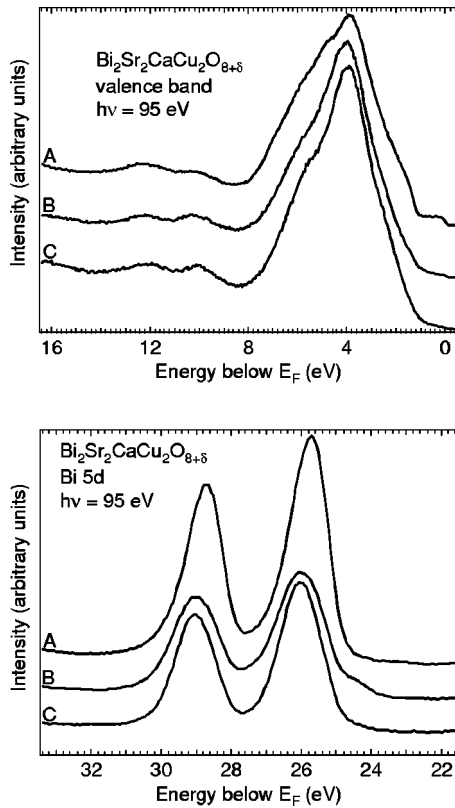


FIG. 2. Photoemission spectra of the valence band (top) and of the Bi 5*d* level (bottom) of the cleaved surface of a $\text{Bi}_2\text{Sr}_2\text{CaCu}_2\text{O}_{8+\delta}$ single crystal. The spectra were recorded from regions A, B, and C indicated in Fig. 1.

contrast is reversed in the two images, which clearly indicates its spectroscopic origin. The valence band and Bi 5*d* level spectra from the three regions are displayed in Fig. 2. Regions B and C are characterized by a lower spectral intensity close to the Fermi edge, which indicates that they are poorer in oxygen than region A.^{9,10} This is further confirmed by the behavior of the feature at 1.5 eV below E_F which is related to oxygen states in the Cu-O layers.^{9,10} This feature is not visible in regions B and C, suggesting the presence of oxygen vacancies in the Cu-O planes. Another indicator is the Bi 5*d* level which is shifted by about 0.3 eV to higher binding energy in regions B and C. Since extrastochiometric oxygen dopes the system with holes, the removing of oxygen atoms will reduce the hole concentration with a consequent shift of the chemical potential. In region B a second component at lower binding energy is present in the Bi 5*d* spectrum. It is assigned to metallic Bi arising from the partial disruption of the BiO surface.¹¹ The length scale of the observed inhomogeneities was determined by acquiring a patchwork of images which is displayed in Fig. 3 (size $300 \times 300 \mu\text{m}^2$). A frame indicates the portion of the surface displayed in the images of Fig. 1. It can be seen that region A surrounds region C, whose size is of the order of $0.3 \times 0.25 \text{ mm}^2$, while region B is only present at the bottom-left border between A and C. A few fault-shaped topographic defects are clearly recognizable in the top-right part of Fig. 3, but they appear not to be correlated with the chemical inho-

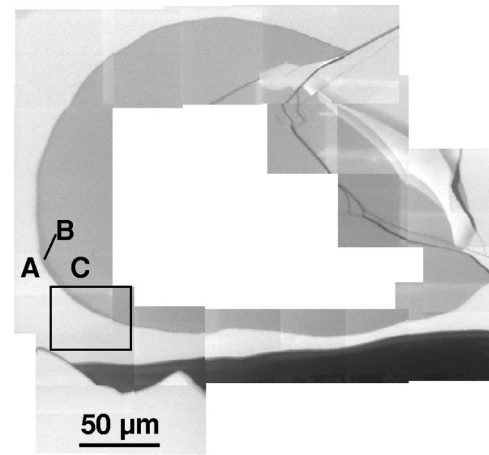


FIG. 3. Photoemission image of the cleaved surface of a $\text{Bi}_2\text{Sr}_2\text{CaCu}_2\text{O}_{8+\delta}$ single crystal. The size is $300 \times 300 \mu\text{m}^2$. The image was acquired detecting photoelectrons from 25.90 to 26.06 eV below E_F . A frame indicates the region displayed in Fig. 1.

mogeneities described above: the faults cross both the A and C regions without marking transitions from one region to the other at the two sides of the topographical defects. The observed chemical inhomogeneities seem therefore an intrinsic characteristic of the sample rather than being related to the cleaving process. We addressed the issue of the relative abundance of the different chemical species by acquiring a valence-band spectrum every 0.1 mm in a region of $1.2 \times 1.2 \text{ mm}^2$ adjacent to the one displayed in Fig. 3. None of the spectra resembles the ones found in regions B and C; that is, all of them look similar to the ones taken in region A, exhibiting a visible feature at 1.5 eV below E_F and a well-developed Fermi edge. However, subtle but significant differences between the spectra are present in the relative intensity of the features at 3.9 and 4.8 eV below E_F and in the details of the spectral shape close to the Fermi edge. This effect was pursued in more detail after cleaving the sample again. Figure 4 (top) shows a photoemission image of the new clean surface (size $400 \times 155 \mu\text{m}^2$) acquired detecting electrons in the range from 24.86 to 25.10 eV below E_F . Besides a pronounced dark feature at the right side of the image, which is due to a cleavage defect, the most evident characteristic of the image is the presence of a top dark region and a bottom bright one. At the bottom of Fig. 4 two images (size $60 \times 60 \mu\text{m}^2$) are shown of the surface portion marked by a frame at the top of Fig. 4. They were acquired at two different electron energies in the range of the Bi 5*d* level, namely from 24.86 to 25.10 eV below E_F (left) and 26.06 eV below E_F (right). Four regions labeled A–D can be distinguished. The contrast between the four regions is strongly dependent on the photoelectron energy, which demonstrates its spectroscopical origin. Figure 5 shows the valence band and the Bi 5*d* level spectra of the four regions. The inset of the valence-band spectrum highlights the differences in shape close to the Fermi edge: in the region from 0 to 0.4 eV below E_F a clear loss of spectral weight is observed in regions B and D which is interpreted in terms of a lower oxygen concentration. The Bi 5*d* level spectra appear

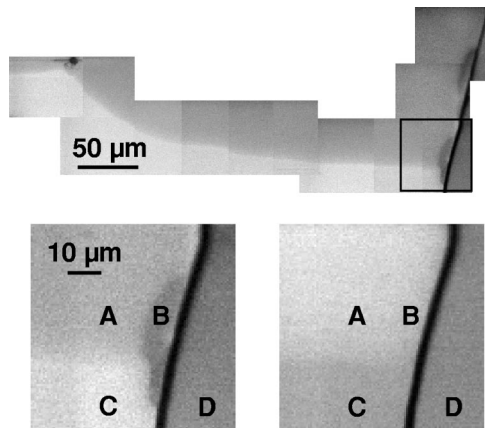


FIG. 4. Top: photoemission image of the cleaved surface of a $\text{Bi}_2\text{Sr}_2\text{CaCu}_2\text{O}_{8+\delta}$ single crystal. The size is $400 \times 155 \mu\text{m}^2$. The image was acquired detecting photoelectrons from 24.86 to 25.10 eV below E_F . Bottom: photoemission images acquired at the surface portion indicated by a frame in the top image. The size is $60 \times 60 \mu\text{m}^2$. The two images were acquired at two different energies of the Bi 5d level: from 24.86 to 25.10 eV below E_F (left) and 26.06 eV below E_F (right), respectively. The four regions labeled A, B, C, and D clearly exhibit different contrast properties in the two images.

in the following order of increasing binding energy: C, D (0.06 eV), A (0.07 eV) and B (0.11 eV), where the numbers in brackets give the shift with respect to the spectrum measured in region C. Therefore, the classification of the four regions by oxygen content is not perfectly correlated to a sequence of increasing binding energy in the Bi 5d spectra as expected on the basis of the simple chemical potential shift arguments explained above. This indicates that other mechanisms, which are not clear at this stage, can induce spatially dependent shifts of the Bi 5d level. We note that in our photoemission microscopy study the Bi 5d level proved to be a very sensitive indicator of the presence of chemical inhomogeneities by exhibiting energy shifts or intensity variations and, due to its high count rate, was therefore preferentially used for image acquisition.

To conclude, we performed photoemission microscopy measurements on cleaved surfaces of a $\text{Bi}_2\text{Sr}_2\text{CaCu}_2\text{O}_{8+\delta}$ single crystal. The sample had been characterized by standard spatially averaged techniques such as LEED and ARPES and exhibited state-of-the-art quality standards.⁸ Spectromicroscopical inspection reveals that the photoemission features change depending on the position on the sample, which is possibly due to an inhomogeneous distribution of the extrastochiometric oxygen. The amount of extra stoichiometric oxygen controls the hole doping of the compound and hence the superconductivity.

This is particularly important for the high energy resolution investigations of the electronic properties (by ARPES)

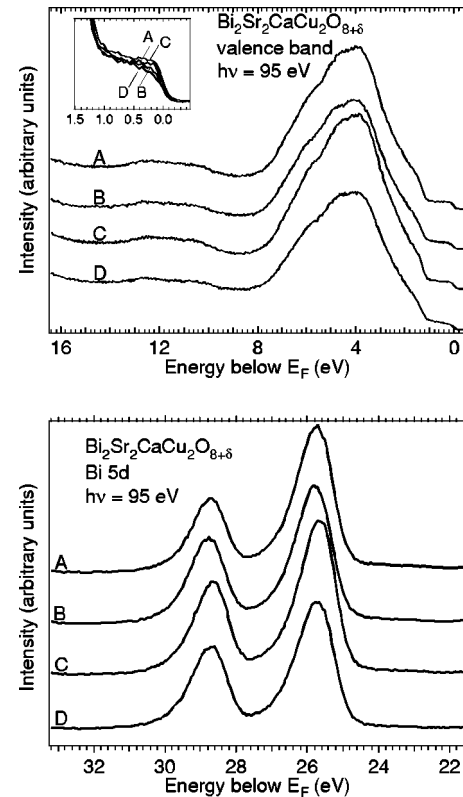


FIG. 5. Photoemission spectra of the valence band (top) and of the Bi 5d level (bottom) of the cleaved surface of a $\text{Bi}_2\text{Sr}_2\text{CaCu}_2\text{O}_{8+\delta}$ single crystal. The spectra were recorded from regions A, B, C, and D indicated in Fig. 4.

both in the normal and in the superconducting states since photoelectrons are collected from macroscopic regions on the sample (size ~ 0.1 – 1 mm). We showed that homogeneous regions exist which extend for several hundreds of μm (see Fig. 5), implying that not necessarily all ARPES data are affected by inhomogeneities. However, we claim that the possible presence of spatial variations should always be considered in the interpretation of area integrated results and is perhaps one explanation for the widely known problem of inconsistent results obtained on nominally identical samples.

The size of the detected features is in some cases higher than the sample thickness. Therefore, it would be interesting to establish whether these features are confined to the cleaved surface they are detected on, or whether they are a cut of a three-dimensional region in the bulk of the $\text{Bi}_2\text{Sr}_2\text{CaCu}_2\text{O}_{8+\delta}$ single crystal.

The authors are indebted to F. Barbo, G. Sandrin, and D. Corso for their valuable technical assistance. This work was supported by the Swedish Research Council and the Royal Swedish Academy of Sciences.

*Electronic mail: bertolo@elettra.trieste.it

¹J. G. Bednorz and K. A. Müller, Z. Phys. B: Condens. Matter **64**, 188 (1986).

²B. N. J. Persson and J. E. Demuth, Phys. Rev. B **42**, 8057 (1990).

³N. Schroeder, S. Weiss, R. Böttner, S. Marquardt, S. Ratz, E. Dietz, U. Gerhardt, G. Ecke, H. Röbner, and Th. Wolf, Physica C **217**, 220 (1993).

⁴P. Almás, T. Dell'Orto, C. Coluzza, J. Almeida, G. Margari-

- tondo, Y. Y. Xue, R. L. Meng, and C. W. Chu, *J. Appl. Phys.* **76**, 1100 (1994).
- ⁵Y. Hwu, C. Y. Tung, J. Y. Pieh, S. D. Lee, P. Alméras, F. Gozzo, H. Berger, G. Margaritondo, G. De Stasio, D. Mercanti, and M. T. Ciotti, *Nucl. Instrum. Methods Phys. Res. A* **361**, 349 (1995).
- ⁶A. A. Zakharov, U. Johansson, M. Leandersson, H. Nylén, M. Qvarford, I. Lindau, and R. Nyholm, *Phys. Rev. B* **56**, R5755 (1997).
- ⁷F. Barbo, M. Bertolo, A. Bianco, G. Cautero, S. Fontana, T. K. Johal, S. La Rosa, G. Margaritondo, and K. Kaznachejev, *Rev. Sci. Instrum.* **71**, 5 (2000).
- ⁸A. A. Zakharov, M. Leandersson, A. Y. Matsuura, I. Lindau, and R. Yoshizaki, *Physica C* **353**, 123 (2001).
- ⁹D. M. Ori, A. Goldoni, U. del Pennino, and F. Parmigiani, *Phys. Rev. B* **52**, 3727 (1995).
- ¹⁰A. Goldoni, V. Corradini, L. Šiller, U. del Pennino, and F. Parmigiani, *Surf. Sci.* **372**, 329 (1997).
- ¹¹S. Söderholm, M. Qvarford, H. Bernhoff, J. N. Andersen, E. Lundgren, R. Nyholm, U. O. Karlsson, I. Lindau, and S. A. Flodström, *J. Phys.: Condens. Matter* **8**, 1307 (1996), and references therein.